

# Trim Drag, Tail Sizing, and Soaring Performance

Ilan Kroo  
NASA Ames Research Center

## ABSTRACT

The requirements of longitudinal stability and trim necessitate small horizontal tail surfaces on conventional sailplanes. Although the penalties in weight and drag associated with sailplane trim requirements are smaller than in those of most other aircraft, they can be significant to the soaring performance of modern sailplanes.

In this paper, the increments in "trim drag" due to induced drag, increased wing profile drag, and wetted area changes are evaluated for standard-class sailplanes. Airfoil section data, combined with a simple method for computing trimmed induced drag of wing/tail systems, are used to compute total trim drag over the entire flight regime, illustrating the effects of circling flight, airfoil pitching moment, and static margin changes.

An investigation of the effects of tail size, aspect ratio, position, and wing lift distribution shape, suggests methods by which trim drag may be reduced. Finally, the paper considers the potential of unconventional configurations for reducing trimmed drag.

## Notation

$\bar{\alpha}$ = ratio of tail to wing lift curve slope	R/S = rate of sink
AR = aspect ratio	$\bar{S}$ = tail area ratio, $\frac{S_t}{S_w}$
$b$ = span	sm = static margin based on ref. chord
$\frac{b}{\bar{c}}$ = tail span ratio, $\frac{b_t}{b_w}$	U = flight speed
$\bar{c}$ = reference chord	$x_c$ = distance from c.g. to canard a.c. in ref. ch
$C_{Dp}$ = profile drag coefficient	$\sigma$ = interference factor (Ref. 7)
$C_L$ = lift coefficient	$\phi$ = bank angle
$C_{L\alpha}$ = lift curve slope	$\mu$ = relative mass, $\frac{2m}{\rho S \bar{c}}$
$C_{mac}$ = pitching moment coefficient about aerodynamic center	$\eta_{ac}$ = spanwise position of a.c. in semispans
$D_i$ = induced drag	$\eta_{CL}$ = spanwise position of lift centroid in semispans
$e_i$ = induced drag span efficiency	$\Lambda$ = quarter chord sweep
$i_c$ = effective canard incidence angle	
J = performance index	
L = lift	
$\frac{L}{\bar{l}}$ = tail (or canard) lift ratio, $\frac{L_t}{L_w}$	
$\bar{l}$ = distance from wing a.c. to tail a.c. in ref. chords	
Q = pitching rate (rad/sec)	
q = dynamic pressure	
q̄ = nondimensional pitching rate $\frac{Qc}{2U}$	

## Subscripts

t	tail or canard
w	wing
turn	value in 61m (200ft) radius turn
100	value at 100 kts
base	value for baseline design

## INTRODUCTION

Although the major role of the horizontal tail is to assure aircraft controllability and satisfactory handling qualities, its influence on performance is receiving increasing attention. On transport aircraft, horizontal tails with twenty to thirty-seven percent of the wing area carry downloads of three to five percent of the aircraft's weight in cruise. The requirement for stability and controllability, therefore, amounts to millions of dollars in annual fuel costs. While controllability requirements for sailplanes are less stringent and fuel costs somewhat lower, the penalty due to trim is still measurable.

Structural weight and landing  $C_{Lmax}$ , for example, are much less important for competition sailplanes with fixed span and non-critical field length constraints. Large tail arms, small center of gravity ranges, and low speed operation make a sailplane's drag penalty due to trim lower than almost any other aircraft type. Nonetheless, even this effect can be important -- 9 meters (30 feet) per minute becomes noticeable after a few minutes.

Several previous papers (Refs. 1-5) deal with trim drag calculations and attempts to reduce the trim penalty. Refs. 1-3 address the problem of sailplane tail design. In this paper, various contributors to trim drag are analyzed, and the importance of static margin, section pitching moment, and wing lift distribution are assessed in straight and circling flight. The analysis tools are then applied to the calculation of optimal tail size and the evaluation of unconventional (canard and tailless) designs.

### SAILPLANE DRAG DUE TO TRIM

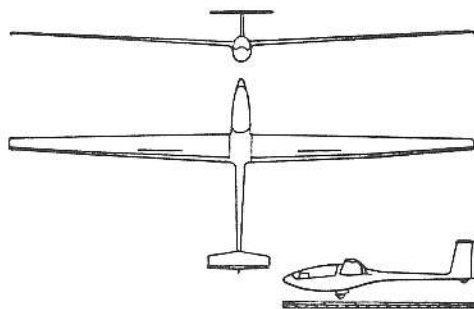
Sources of drag directly related to the trim requirement include:

- Induced drag of the wing/tail system
- Parasite drag of the tail
- Increased wing profile drag due to higher  $C_L$  with tail download

The aircraft empty weight is also increased by the horizontal tail loads,

but this usually has no important effect on the trimmed polar. The following sections illustrate the magnitude of each of these effects for the standard-class sailplane of Fig. 1.

Fig. 1 Conventional, Baseline 15-m, Sailplane



### 1. Tail Load

Before any aspect of trim drag may be computed it is necessary to estimate the load carried by the tail as a function of airspeed. This is determined by computing the c.g. for a given static margin,  $sm$ , and requiring that the pitching moment about the c.g. be zero (trim). The tail lift ratio is (see nomenclature):

$$\bar{L} = \frac{L_t}{L_w} = \frac{\bar{a}\bar{S}l - (1 + \bar{a}\bar{S})(sm - \frac{C_{m0}}{C_{Lw}})}{1 + (1 + \bar{a}\bar{S})sm} \quad (1)$$

The ratio of lift curve slopes depends on wing and tail aspect ratios, planforms, and interference effects, and was computed here by a multiple surface, extended lifting line method (cf. Ref. 6).

Because of the airfoil's negative pitching moment, the tail download required to trim increases with airspeed. At minimum sink speed, the tail contributes small positive lift; at high speeds, however, the tail carries a substantial download (6% at 100 kts).

### 2. Induced Drag

The induced drag of the aircraft depends on surface planforms, twist distributions, fuselage interaction, and

relative position of the wing and tail. For the purposes of this analysis, however, the lift distribution will be taken to be nearly elliptical over each surface. In this case, the Prandtl biplane equation may be used to compute the induced drag of the wing/tail system:

$$D_i = \frac{L_w^2}{q\pi b_w^2} + \frac{2L_w L_t}{q\pi b_w b_t} \sigma + \frac{L_t^2}{q\pi b_t^2} \quad (2)$$

The interference factor,  $\sigma$ , accounts for the interference between the wing and tail. It depends on the vertical separation between the surfaces and the ratio of their spans and is presented in Ref. 7.

The span efficiency is the ratio of the induced drag of a single elliptically loaded wing to the induced drag of this system and is given by:

$$\epsilon_i = \frac{(1 + \bar{L})^2}{1 + \frac{2\sigma\bar{L}}{b} + \frac{\bar{L}^2}{b^2}} \quad (3)$$

The span efficiency thus varies considerably with the ratio of the tail span to wing span,  $\bar{L}$ , whenever the tail carries a significant load. When the tail is lifting,  $\epsilon_i$  can exceed 1, but down-loaded tails produce large induced drag penalties even with relatively small loads.

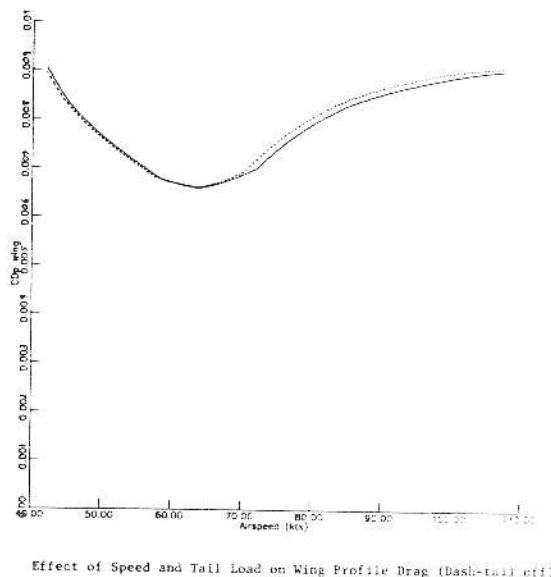
For the example standard-class sailplane, the span efficiency drops from about 0.996 at 50 kts to 0.806 at 100 kts. The increase in total drag due to the induced drag penalty is about .2% at 50 kts and .9% at 100 kts.

### 3. Wing Profile Drag

The wing profile drag varies with Reynolds number and lift coefficient. If the tail carries any load, the wing  $C_L$  at any given speed will be changed and hence its drag will change.

Because the section polar is relatively flat in the region of interest, changing the wing  $C_L$  due to tail download does not change the wing section drag appreciably. The wing profile drag does vary considerably over the speed range however, as shown in Fig. 2. The dashed curve represents  $C_{Dp\text{wing}}$  in the absence of tail load; the

Fig. 2 Effect of Tail Load on Wing  $C_{Dp}$



solid line includes the tail's influence. Since the high speed portion of the sink rate polar lies at a  $C_L$  below the drag bucket of this unflapped section, the tail load actually reduces the wing profile drag at speeds above about 60 kts.

### 4. Tail Profile Drag

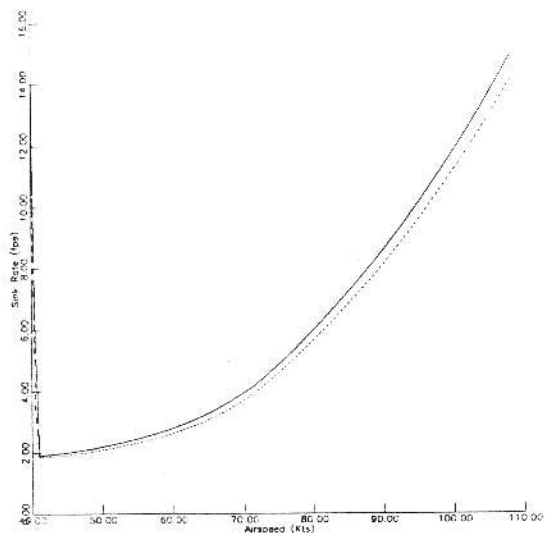
The tail's profile drag produces the greatest influence on total drag. With 10% of the area of the wing, a horizontal tail typically contributes 7% of a high performance sailplane's total flat plate drag area. Although the section need not generate high lift coefficients and, therefore, may be thin with little camber, the low Reynolds number of tail surfaces leads to tail drag coefficients similar to those of the wing.

Several investigations of tail section characteristics have been published (Refs. 2, 8), including the effects of elevator deflection. In this analysis the horizontal tail is assumed to be an all-moving surface with drag characteristics based on the FX-71-L-150 (Ref. 8) at the appropriate Reynolds number.

## 5. Net Effect of the Horizontal Tail on Sink Rate Polar

The importance of these effects and the variation with forward speed is illustrated by the computed sink rate polars in Figure 3. The solid line represents

Fig. 3 Computed Sink Rate Vs. Airspeed  
Solid - Trimmed, Dash - Tail-Off



the sink rate of the complete, trimmed aircraft while the dashed line indicates the hypothetical polar of the same sailplane, untrimmed, with no horizontal tail.

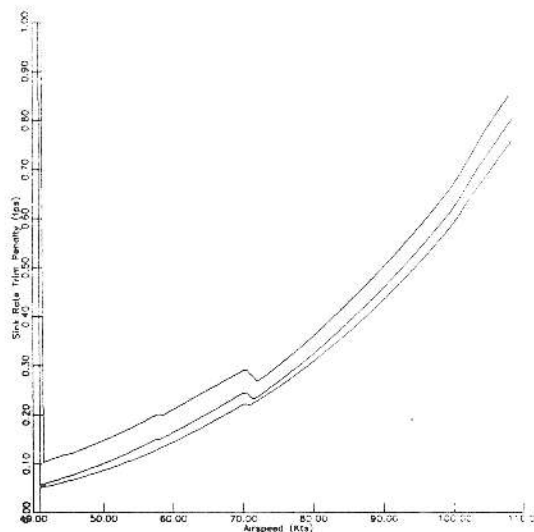
The penalty due to the trim requirement increases with speed, primarily because of the increasing importance of parasite drag at high speeds. Since the unflapped FX-67-K-150 section begins to leave the laminar drag bucket at higher speeds, the trim penalty reaches a maximum at about 70 kts where a 6% increase in sink rate may be attributed to the requirement for trim.

### STABILITY AND TRIM PARAMETERS -- EFFECTS ON TRIMMED DRAG

#### 1. Static Margin

The sailplane of Figure 1 permits a c.g. location from 20% to 40% of the wing's mean aerodynamic chord. This corresponds to a static margin of .14 to .34 excluding the destabilizing effect of the fuselage. In Figure 4 the

Fig. 4 Effect of Static Margin on Trim Drag  
sm = .14, .24, .34

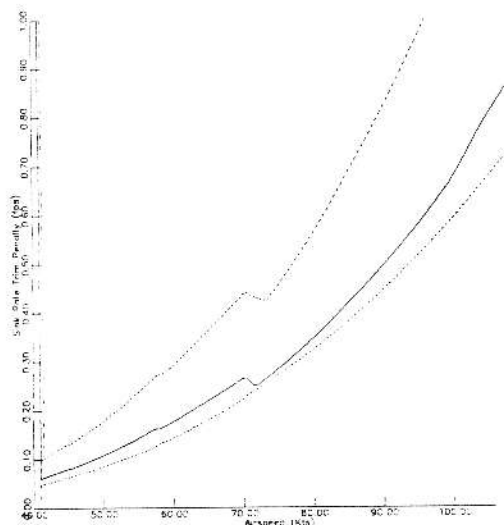


difference between trimmed and untrimmed (tail-off) polars is plotted vs. airspeed for forward, mid, and aft c.g. positions. (The unusual 'kink' in the curves is related to some anomalies in the FX-67-K-150 data at the lower end of the drag bucket in this Reynolds number range. It is apparent only because of the expanded vertical scale of these figures.) The general increase in trim penalty with airspeed (due to larger downloads and increased importance of parasite drag), is accentuated somewhat by the forward c.g. positions, but not to any great extent. In fact, the difference in these sink rate polars is barely noticeable, indicating that no significant savings in trim drag is possible by simply reducing static stability.

#### 2. Section Pitching Moment

The section pitching moment determines the tail load at high speeds. Figure 5 shows the influence of this parameter on sink rate penalty due to trim. Reducing the section moment from 0 to -0.1 increases the trim penalty somewhat, but decreasing the  $C_{mo}$  to -0.2 has a profound effect over most of the speed range. Although the profile drag characteristics of the section were given and the wing was assumed unflapped, the results indicate that

Fig. 5 Effect of Section Moment on Trim Drag  
 $C_{m0} = 0, -1, -2$



upward flap deflection is important in reducing trim drag as well as improving the section drag at high speeds. Similarly, low speed flap deflection produces diminishing returns since trim drag increases with flap deflection.

## CIRCLING FLIGHT

### 1. Tail Load to Trim

In a steady, descending turn, the effective curvature of the flow introduces pitch damping and changes the tail load required for trim. If the wing is unswept, the major influence on tail trimming load at a given  $C_L$  is an effective increase in wing section moment:

$$\Delta C_{m0} = -\frac{\hat{q}}{q} \frac{\pi}{4} \quad (4)$$

with:

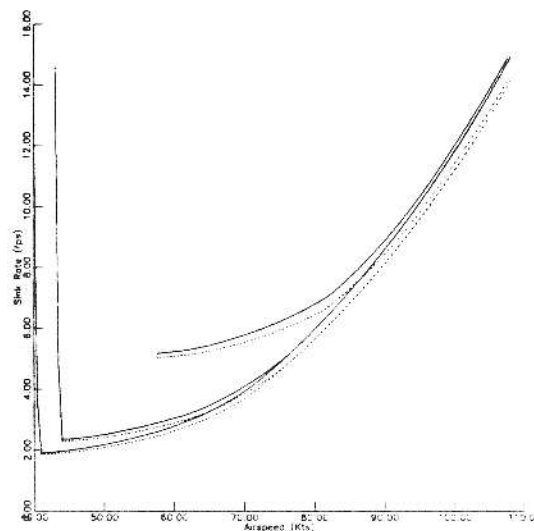
$$\hat{q} = \frac{C_L \sin^2 \phi}{2\mu}$$

For aircraft with low values of  $\mu$  (hang gliders, ultralight sailplanes, etc.) this effect can be large (Ref. 9). But for a 15-m sailplane, even a 60 degree bank at low speeds produces a change in  $C_{m0}$  of less than .01. The major effect of flow curvature is a change in tail incidence, not trimming load. While this may be important for sailplanes with fixed incidence tails and elevators, it is not considered here.

## 2. Trim Drag in Circling Flight

Although the tail load to trim at a given  $C_L$  is not appreciably changed in a turn, the relative importance of induced drag increases. The low speed polar is modified as shown in Figure 6 for bank angles of 0, 30, and 60 degrees. Trim drag also rises but remains a small effect for typical c.g. positions and tail sizes, even for the relatively high bank angles.

Fig. 6 Computed Sink Rate Vs. Airspeed  
 Solid - Trimmed, Dash - Tail-Off, Bank = 0,30,60



Effect of Bank Angle on Sink Rate

## REDUCING TRIM DRAG

The analysis indicates that small drag savings are possible by reducing the static margin utilizing airfoils with low section pitching moments. However, except perhaps in turns with flaps deflected, the changes are so small that probable degradations in handling qualities with more aft c.g. positions would overwhelm any improvements.

Another technique for reducing trimmed induced drag involves reducing the vertical separation between the wing and tail and/or modifying the shape of the wing lift distribution. In theory, one can eliminate all induced drag penalties by modifying the wing lift distribution to cancel the vortex drag of the tail (Ref. 7). In practice, this

cancellation is not perfect and except for canard configurations, this technique does not lead to substantial drag savings.

Thus, with typical wing and tail geometries, little can be done to reduce the small drag penalty due to trim. We next consider the role of tail size and aspect ratio -- parameters which do have an important impact on trim drag.

### TAIL SIZING

Tail area, tail span, and wing area are the primary variables affecting the trimmed drag of 15-m sailplanes. The conventional approach to surface sizing involves selecting the wing parameters and adding a horizontal tail which is just large enough to ensure adequate control. But, this does not always lead to tail designs with minimum drag.

The predominance of tail profile drag in the drag penalty due to trim suggests that increasing tail area will increase trimmed drag. Although this is true when the wing geometry is fixed, sailplanes with larger tails require smaller wing areas. The net differences in performance among sailplanes with various tail sizes and optimized wings are not obvious.

High speed performance is strongly influenced by total surface area, which is, in turn, determined by the requirement for low speed soaring capability. Tails with relatively large spans carrying positive lift provide an induced drag advantage which is especially important at low speeds. One can, however, go too far. Tails of very large span (tandems) are not advantageous for most aircraft since structural weight penalties outweigh the advantage in span efficiency. For sailplanes it is not structural weight, but Reynolds number effects which eliminate tandem designs from contention. To determine when this Reynolds number penalty overcomes the increase in span efficiency, the soaring performance of sailplanes with optimal wing areas was computed for various tail geometries.

#### 1. Wing/Tail Optimization

The methods discussed on previous pages

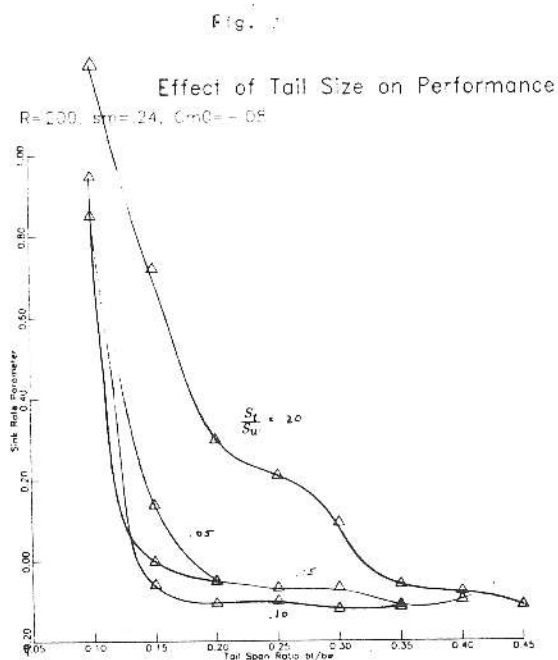
were applied to the study of sailplanes with differing wing area, tail area, and tail span. The FX-67-K-150 section data were used to predict wing profile drag and FX-71-L-150 data were applied to the tail in most cases. When the tail Reynolds number became lower than 700,000 over part of the polar, the Eppler 201 data from Ref. 10 (which includes data for Reynolds numbers down to 60,000) was used. These data were linearly interpolated vs.  $C_L$  and Reynolds number. Tail loads, wing and tail  $C_L$ 's, and induced and profile drags were calculated over the entire polar as described previously.

Objective: Since both high and low speed portions of the polar are critical to soaring performance, it is not possible to consider solely the minimum drag or the sink rate at a given speed. Several optimization studies (cf. Ref. 11) have used average cross-country cruising speed as the measure of performance. This is a desirable approach but is sensitive to assumptions regarding interthermal downdraft strength, thermal size, strength, and spacing. Indeed, the optimal sailplane geometry is sensitive to the conditions in which it is to be flown. A simplified index of soaring performance is used in this study. This measure is subject to several problems but captures some of the basic characteristics that determine sailplane performance. The sink rate at 100 kts and in a turn of 61 m (200 ft) radius are included in the following goal function:

$$J = w_1 \frac{\Delta R/S_{100}}{R/S_{100base}} + w_2 \frac{\Delta R/S_{turn}}{R/S_{turnbase}}$$

This goal function is the sum of the fractional increase in minimum sink rate in a 61 m (200 ft) radius turn (at the optimal bank angle) and in straight flight at 100 kts. The baseline values are those of the example sailplane of Fig. 1. Each of the weighting factors,  $w_1$  and  $w_2$ , are increased when the sink rate exceeds the baseline since spectacular high speed performance will not compensate for truly inferior turning performance. Interestingly, the results are relatively insensitive to the ratio

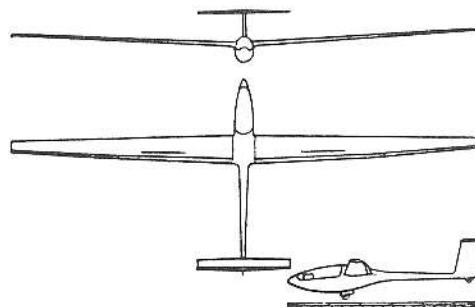
$w_2/w_1$ , and with conventionally-sized tails lead to an optimal wing area of 10 sq m (107 sq ft). Designs with minimum sink rate in straight flight have considerably smaller optimal wing areas, illustrating the importance of modeling turning performance. Results are shown in Fig. 7. The sink rate parameter,  $J$ , is plotted vs. tail span ratio,  $\frac{b_L}{b_w}$  for various tail area ratios,  $\frac{S_L}{S_w}$ .



The figure indicates that although lower aspect ratio tails may produce lower profile drag due to higher Reynolds numbers, the improved low speed, circling performance of the higher aspect ratio tails compensates for this and the optimal horizontal tail seems to have an area of about 10% of the wing area with about 20% of the span (aspect ratio = 9). The optimum is rather flat with tail aspect ratios from 7 to 20 producing little change in the goal function. Aeroelastic effects and structural considerations would suggest selection of the lower tail aspect ratios from 6 to 9. These configurations have slightly smaller (by about 1%) wing areas than the baseline design; they achieve nearly identical high speed performance, and they attain minimum sink rates in a 61 m (200 ft) radius turn of about 3% less than the

base-line. The configuration is shown in Figure 8. These results differ from those of Ref. 3 in which the smallest area tails seemed best.

Fig. 8



Conventional Configuration with "Optimum" Tail

In the present study, substantial penalties are predicted for tails much smaller than 10% of the wing area and penalties for tails with 15% of the wing area are not large. The use of a goal function which includes both circling flight and high speed performance rather than minimum drag accounts for some of the discrepancy between the studies. Additional factors include the explicit dependence of profile drag on wing and tail  $C_L$ , larger static margin, and the use of low Reynolds number airfoils for the higher aspect ratio tails.

Results from the optimization procedure using minimum straight flight sink rate rather than fixed turn radius, lead to optimal tails with aspect ratios of about 4 to 7 and do not yield such a large penalty for smaller tail areas.

Reducing the static margin leads to smaller tails and improved high speed performance. So, while changing the c.g. position of a given aircraft does not make a significant difference to performance, changing the c.g. position and redesigning the aircraft for optimal performance produces larger gains. (The optimal tail with static margin of 0 predicted by this program, has 5% of the wing area, an aspect ratio of 5 and a wing with about 2% greater area than the baseline design. It achieves a 7%

reduction in minimum sink in the 61 m (200 ft) turn and about the same sink rate at 100 kts.)

### UNCONVENTIONAL DESIGNS

Little room for substantial improvement in the trimmed drag of conventional sailplanes appears possible. This has led a number of creative designers to consider radical departures from the conventional configuration (Refs. 12-14). Such unusual designs include canards and swept or unswept tailless aircraft. Although no unconventional design has proven competitive with modern, conventional sailplanes, it is useful to investigate whether this failure is due to a fundamental penalty with such designs or simply poor implementation of the concepts. The following sections constitute a simple look at the potential of such designs for reducing sailplane trimmed drag.

#### 1. Canards

The motivation for canard designs often involves considerations not directly related to aerodynamic performance. Control system simplicity, handling qualities, engine integration (if any), and other less identifiable issues constitute important aspects of configuration selection which are difficult to quantify. Here we consider certain elements of performance of interest to sailplane pilots.

Equation 1 may be used to compute tail (canard) loads for canard configurations as well as aft-tail designs. (Care must be taken in the calculation of lift curve slope ratio to include interference effects of the wing/canard system and the effect of canard section moment.)

For typical canard configurations (with reasonably high aspect ratio, unswept canard surfaces), the required canard lift coefficient is larger than that of the wing. Unlike an aft tail, the canard airfoil must operate over a large range of lift coefficients. This leads to challenges in low Reynolds number airfoil design (Ref. 15) and

inevitable penalties in profile drag. The relatively large lift carried by a canard may also lead to induced drag penalties. A canard with 40% of the wing span, carrying 35% of the wing's lift, achieves a span efficiency of only .74 (Eqn. 3). By employing a more optimal distribution of wing lift, this penalty may be reduced somewhat (Ref. 7). However, the lift distribution required to achieve minimum induced drag is highly non-uniform. This leads to variations in section lift coefficient over the wing so that airfoil section tailoring (to obtain the desired distribution and maintain a wide range of wing  $C_L$ 's over which laminar flow prevails) is a necessity for such designs.

The effect of circling flight on the canard or tail load to trim is similar for canard and conventional designs. For fixed incidence canards, however, the effective incidence change can be important. The incidence change at the canard is  $\Delta i_c = 2\hat{q}x_c$ . Using the expression for  $q$  from Ref. 9,

$$\Delta i_c = \frac{x_c C_L \sin^2 \phi}{\mu}$$

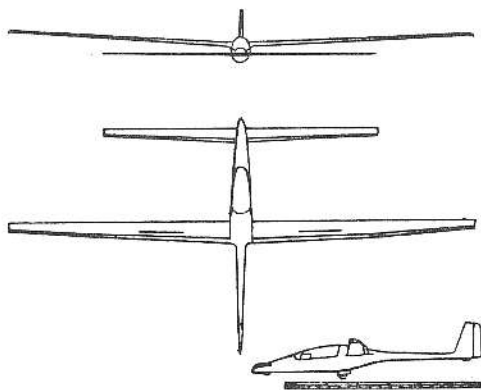
At low speeds, with moderate bank angles, the effective incidence change is about one or two degrees. The canard must be designed to achieve reasonable maximum trimmed  $C_L$ 's in level flight and in turns with lower effective incidence. This presents difficulties which increase as the relative mass decreases. To assess the basic interactions of the wing and canard in terms of potential sailplane performance, details of wing twist, canard incidence, and profile drag variations over the wing are ignored. The wing profile drag is computed based on FX-67-K-150 data while the canard is assumed to follow the predicted polar of Eppler's 1233 section with flap.\*

\* Such a canard design has an advantage over the standard-class, conventional sailplane since the "elevator" on the forward surface acts as a flap while the wing of both designs is required to be "clean."

Induced drag is assumed half-way between the results for elliptical loading (Eqn.3) and optimal loading (Ref. 7).

The optimization procedure used in the tail sizing studies leads to the configuration pictured in Figure 9 with the sink rate polar prediction in Figure 10. This configuration achieves about the same sink rate at 100 kts as the conventional configuration but suffers higher sink rates at low speeds. The lower wing  $C_L$  does, however, lower the

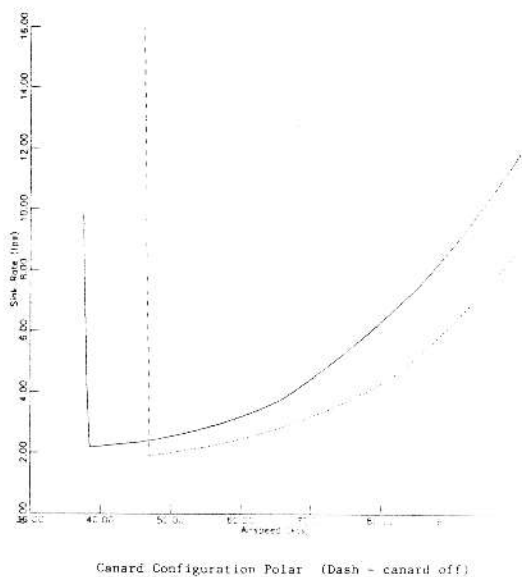
Fig. 9



"Optimized" Canard Configuration

Fig. 10

Computed Sink Rate vs. Airspeed  
Canard  $b_0/b_w = 6$ ,  $S_0/S_w = .4$ ,  $S_w = 80$



speed for minimum sink so that this configuration achieves a minimum sink rate in a 61 m (200 ft) turn of 1.5% less than the conventional design. The sink rate penalty below 100 kts in straight flight, combined with difficulties in obtaining low profile drag over the wing span, make this potential advantage in turning flight seem small. The change in effective canard incidence in turning flight, and a margin of safety against aft surface stall, would probably result in reduced turning performance.

Because of the large fraction of lift carried by the canard ( $\frac{L_c}{L_w} = .5$ ), the

performance of this design is more sensitive to static margin changes than the conventional configuration so that some improvement might be expected if reductions in static stability were permitted. Nevertheless, the results are neither very encouraging (the performance is not substantially better than the conventional design) nor very discouraging (the performance is not much worse). If carefully executed, a canard configuration might make an acceptable, although probably not an exceptional, high performance sailplane.

## 2. Tailless Sailplanes

It is, of course, possible to trim a sailplane without a tail or canard by producing a pitching moment about the wing's aerodynamic center of:

$$C_{mac} = \sigma m C_L$$

Several such existing and hypothetical designs are motivated by the apparent performance advantages due to the elimination of a separate trimming surface.

Two methods may be employed to achieve the required pitching moment about the wing aerodynamic center without a tail. First, an airfoil section with positive pitching moment may be used. Reducing aft camber (by means of a trailing edge control surface) can lead to pitching moments of the required magnitude; however, the penalty in profile drag at higher  $C_L$ 's is large. Data on airfoils with large positive pitching moments designed for low drag are not

available and one might do substantially better than existing sections. However, the data of Ref. 8, for airfoils with flaps, suggests that to provide a static margin of .2 at a  $C_L$  of 1.0 ( $C_{m0} = .2$ ) would entail completely unacceptable drag penalties.

A more reasonable approach involves the use of sweep and wing twist to generate positive moments about the wing a.c.. As with wing/tail combinations, a simple method for computing the minimum, trimmed, induced drag of swept, tailless configurations may be used to assess their performance potential without detailed consideration of the actual distributions of twist. The condition for trim may be written:

$$C_{mac} = \sigma m C_L$$

and 
$$C_{mac} = C_{m02D} + \frac{C_L AR \tan \Lambda}{2} (\eta_{ac} - \eta_{CL})$$

So, for trim: 
$$\eta_{CL} = \eta_{ac} - \frac{2(\sigma m - \frac{C_{m02D}}{C_L})}{AR \tan \Lambda}$$

The spanwise position of the aerodynamic center depends on taper, sweep, and aspect ratio, and may be computed by extended lifting line methods (Ref. 6). Then, the maximum span efficiency is related directly to the position of the lift centroid,  $\eta_{CL}$  (Ref. 16) by:

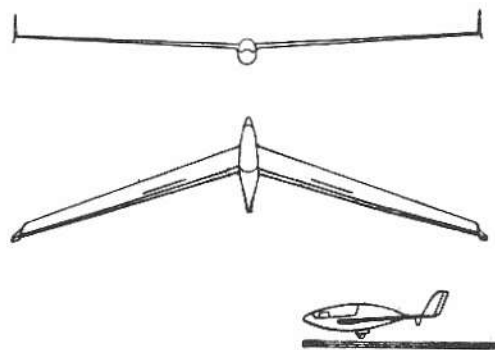
$$e_i = \left[ \frac{9}{2} \pi^2 \eta_{CL}^2 - 12 \pi \eta_{CL} + 9 \right]^{-1}$$

The profile drag also varies with the shape of the lift distribution but, as in the canard case, we ignore this effect in the following analysis. The effect of sweep on the profile drag of these laminar flow sections must be given more careful attention. Recent experiments confirm the existence of large amounts of laminar flow on composite wings with 25 degrees of sweep in this Reynolds number range. However, specific details on the extent of the laminar drag bucket with  $C_L$  are not available. Furthermore, pronounced three-dimensional viscous effects appear on swept wings, making the use of section data inappropriate or, at best, highly approximate. Finally, aeroelastic deformations of this high aspect ratio, swept wing will reduce the static margin at high speeds and unusual

flutter modes are among the many unknowns associated with such a design.

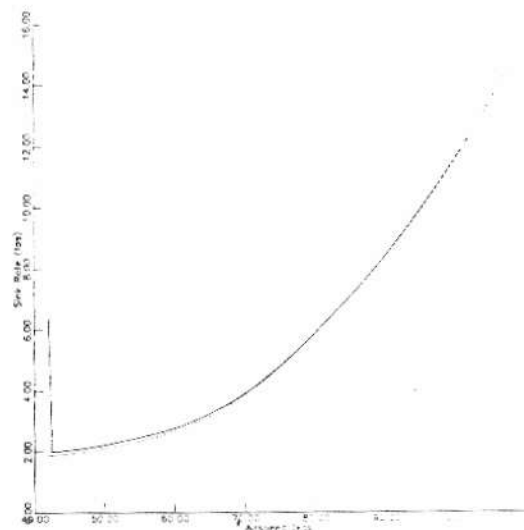
With these uncertainties, the same analysis and performance optimization of tail and canard sizing was applied to the swept, tailless configuration. Figures 11, 12 illustrate the resulting configuration and sink rate polar.

Fig. 11



"Optimized" Tailless Configuration

Fig. 12

Computed Sink Rate vs. Airspeed  
Tailless, Sweep=20, taper=7

Tailless Sailplane Polar (Dash - Untrimmed)

As in the canard case, some performance advantages are predicted -- but they are small, especially in light of the assumptions required in the

analysis. A second similarity with the canard case is the possible performance improvement with reduced static margin or  $C_{m0}$ .

### CONCLUSIONS

This broad look at trimmed, soaring performance of a variety of possible high performance sailplane configurations suggests the following:

Trim drag penalty due to the requirement for longitudinal stability and trim constitutes a small, but noticeable part of a conventional sailplane's drag.

Changes in static margin, section  $C_{m0}$ , and tail vertical position produce small changes in trimmed drag, important only with very large static margins or large flap deflections. The effects are accentuated in circling flight.

Tails sized for optimal performance in combined circling flight and high speed cruise have larger spans (and aspect ratios) than those based on straight flight calculations. Such tails should also improve performance at forward c.g. positions.

Based on the assumptions of these analyses, canard designs and swept, tailless sailplanes may rival the performance of conventional sailplanes, but in practice will probably involve some performance compromises. Unless reductions in static stability are possible, considerations other than trimmed drag must recommend these unconventional designs.

### REFERENCES

1. Bauman, J.T.: Effect of Stabilizer Lift on Sailplane Performance, Technical Soaring, Vol. I, No. 4.
2. Althaus, D.: Measurements on Airfoils with Flaps at Medium Reynolds Numbers, Technical Soaring, Vol. V, No. 2, 1978.

3. Mayland, K.: Optimum Tail Plane Design for Sailplanes, Science and Technology of Low Speed and Motorless Flight, NASA CP 2085, 1979.
4. Laitone, E.: Ideal Tail Load for Minimum Aircraft Drag, Journal of Aircraft, 1978.
5. Sachs, G.: Minimum Trimmed Drag and Optimum C.G. Position, Journal of Aircraft, 1978.
6. Schlichting, H. and Truckenbrodt, E.: Aerodynamics of the Airplane, McGraw-Hill Book Co., 1979.
7. Kroo, I.: Minimum Induced Drag of Canard Configurations, Journal of Aircraft, Sept. 1982.
8. Althaus, D. and Wortmann, F.X.: Stuttgarter Profilkatalog I, Institut für Aerodynamik und Gasdynamik, der Universität Stuttgart.
9. Kroo, I.: Aerodynamics, Aeroelasticity, and Stability of Hang Gliders Thesis, Stanford University, 1983.
10. Althaus, D.: Profilpolaren Für Den Modellflug, Institut für Aerodynamik und Gasdynamik, der Universität Stuttgart.
11. Helwig, G.: Wing Shape Optimization for Maximum Cross-Country Speed, Technology and Science of Low Speed and Motorless Flight, NASA CP-2085, 1979.
12. The Homebuilt Sailplane Design Contest, Soaring Society of America, 1982.
13. McMasters, J.H.: "Flying the Altostratus I", Soaring, Feb. 1981.
14. Gyorgyfalvy, D.: Performance Analysis of the Horten IV Flying Wing, VIII OSTIV Congress, 1960.
15. Eppler, R.: Some New Airfoils, Technology and Science of Low Speed and Motorless Flight, NASA CP-2085, 1979.
16. Jones, R.T.: The Spanwise Distribution of Lift for Minimum Induced Drag of Wings Having a Given Lift and Root Bending Moment, NACA TN 2249, 1950.